Computers in Biology and Medicine 113 (2019) 103416

Contents lists available at ScienceDirect

Computers in Biology and Medicine

journal homepage: www.elsevier.com/locate/compbiomed

Large-scale ensemble simulations of biomathematical brain arteriovenous malformation models using graphics processing unit computation

Mika S. Jain[a,b], Huy M. Do[c,d], Max Wintermark[c,e], Tarik F. Massoud[c,*]

[a] Department of Physics, Stanford University School of Humanities and Sciences, Stanford, CA, USA
[b] Department of Computer Science, Stanford University School of Engineering, Stanford, CA, USA
[c] Division of Neuroimaging and Neurointervention, Department of Radiology, Stanford, CA, USA
[d] Department of Neurosurgery, Stanford, CA, USA
[e] Department of Neurology and Neurological Sciences, Stanford University School of Medicine, Stanford, CA, USA

ARTICLE INFO

Keywords:
Biomathematical model
Brain AVM
Hemorrhage
Hemodynamics
Network
Nidus
Rupture

ABSTRACT

Background: Theoretical modeling allows investigations of cerebral arteriovenous malformation (AVM) hemodynamics, but current models are too simple and not clinically representative. We developed a more realistic AVM model based on graphics processing unit (GPU) computing, to replicate highly variable and complex nidus angioarchitectures with vessel counts in the thousands—orders of magnitude greater than current models.

Methods: We constructed a theoretical electrical circuit AVM model with a nidus described by a stochastic block model (SBM) of 57 nodes and an average of 1000 plexiform and fistulous vessels. We sampled and individually simulated 10,000 distinct nidus morphologies from this SBM, constituting an ensemble simulation. We assigned appropriate biophysical values to all model vessels, and known values of mean intravascular pressure (P_{mean}) to extranidal vessels. We then used network analysis to calculate P_{mean} and volumetric flow rate within each nidus vessel, and mapped these values onto a graphic representation of the nidus network. We derived an expression for nidus rupture risk and conducted a model parameter sensitivity analysis.

Results: Simulations revealed a total intranidal volumetric blood flow ranging from 268 mL/min to 535 mL/min, with an average of 463 mL/min. The maximum percentage rupture risk among all vessels in the nidus ranged from 0% to 60%, with an average of 29%.

Conclusion: This easy to implement biomathematical AVM model, allowed by parallel data processing using advanced GPU computing, will serve as a useful tool for theoretical investigations of AVM therapies and their hemodynamic sequelae.

1. Introduction

Ruptured cerebral arteriovenous malformations (AVMs) are a significant source of morbidity and mortality [1]. An abnormal low-resistance AVM nidus exhibits rapid blood shunting between arterial feeders (AFs) and draining veins (DVs). The consequent global hemodynamic factors contributing to nidus rupture have been studied extensively, but there are currently no practical in vivo techniques to accurately study hemodynamics inside an AVM nidus.

Biomathematical modeling offers an approach to do this theoretically. However, AVM models conceived to date have been extremely simple, usually possessing small numbers of simulated intranidal vessels in rudimentary geometrical arrangements that do not adequately represent the complex network morphologies within large AVMs [2–4]. A true AVM nidus consists of a tightly interwoven complex mesh of microvessels [5] that are typically interconnected, and with innumerable branching points, making these intranidal channels hemodynamically interdependent.

Here we describe a novel computational model of cerebral AVMs based on theoretical electrical network analysis. Recent advances in graphics processing unit (GPU) computing only now permit efficient network analysis and simulations using extremely high nidus vessel numbers. We used high-speed, massively parallel GPU-accelerated computational techniques to develop a more authentic model than available previously, replicating morphologically complex and highly variable AVM nidi. We characterize the model hemodynamics as a prelude to future applications in theoretical simulations of AVM therapy and its complications.

* Corresponding author. Division of Neuroimaging and Neurointervention; Stanford University, 300 Pasteur Drive, Stanford, CA, 94305, USA.
E-mail address: tmassoud@stanford.edu (T.F. Massoud).

https://doi.org/10.1016/j.compbiomed.2019.103416
Received 6 May 2019; Received in revised form 24 August 2019; Accepted 24 August 2019
Available online 27 August 2019
0010-4825/

2. Materials and methods

2.1. AVM hemodynamics

Blood flow within most of the human vasculature consists of a non-Newtonian fluid flowing in a pulsatile nature through viscoelastic tapered tubes. This requires computationally intensive calculations to simulate with high fidelity. However, since blood flow in AVMs and surrounding vasculature is within thin capillary-like vessels downstream of high capacitance vessels, turbulence, pulsatility, and changes in viscosity are negligible. AVM hemodynamics can therefore be described sufficiently by the Hagen–Poiseuille equation,

$$Q = \pi \Delta P r^4 / 8 L \eta, \quad (1)$$

where Q is vessel flow rate, ΔP is the difference in pressure between the ends of the vessel, r is vessel inner radius, L is vessel length, and η is the blood viscosity (η = 3.5 centiPoise). This is analogous to Ohm's law of electricity, $I = V/R_v$, with current I = Q, voltage V = ΔP, and vessel resistance $R_v = 8 L \eta/\pi r^4$. This analogy allows simulation of the fluidic network of blood flow within AVM vasculature using established, matrix-based analysis of electrical networks. If pressure, length, and radius are known for all blood vessels, it is possible to calculate blood flow rate throughout the entire AVM.

2.2. AVM network model

The general merits and drawbacks of electrical network modeling of theoretical cerebral AVMs, as summarized in the Supplementary Discussion, have been published and extensively referenced by Hademenos et al. [6] previously, and these apply here similarly. To achieve a more complex and realistic elaboration on the previously published Hademenos et al. [6] model, which lacked sufficient nidus size and morphological complexity, we introduced two main improvements. First, we increased the number of intranidal vessels—many more vessels than any previously published model. The main advantage of this is that it allowed the performance of simulations within anatomically more faithful representations of AVMs. Second, we introduced extremely high stochastic variability in nidus configurations and complex nidus angioarchitectures, including vessels that connected to more distant nodes. Previous studies have all used AVM networks that were simple planar renderings (see Discussion). Our departure from this was necessary to ensure a degree of complexity in a network model that reflects the true angioarchitecture of human AVMs.

In network analysis, vessels of various radii and lengths are distributed randomly in a dependent manner to resemble a highly disordered frame or network through which fluid will flow. In analogies found in electricity, the circulatory network can be represented by a complex electrical circuit of connected wires with variable resistance through which the current or flow, powered by an electrical power source or pressure gradient, will traverse. Each wire or vessel connection represents a node or a location at which flow converges and diverges. With respect to the AVM, the node resembles the start or end of a vascular branch, e.g., a bifurcation or trifurcation, within the vascular bed.

Thus, we constructed a theoretical electrical network to closely simulate the cerebral circulation containing an AVM. The AVM consisted of four AFs (AF1-AF4), three DVs (DV1-DV3), an isolated fistulous channel of four vessels (from AF2 to DV2), and a random arrangement of nidus plexiform vessels interconnecting 57 nidus nodes (Fig. 1). We defined the nidus angioarchitecture as a stochastic block model (SBM) where plexiform vessels randomly appeared between any two of the nidus nodes with a probability (1000/[*57* choose *2*], i.e., a binomial coefficient of 0.63), resulting in a range from 919 to 1,084, with an average of 1000 plexiform nidus vessels. Importantly, this high variability allows the simulation and study of a vast number of different nidus configurations rather than only one, so that generalizable conclusions could be made about the behavior of diverse AVMs. This model, with exactly 1000 vessels and 57 nodes, has an extraordinarily high number of possible vessel configurations ([*57* choose *2*] choose *1,000*, i.e., a binomial coefficient of 2.03×10^{456}). Next, we performed the simulations on an ensemble of nidus angioarchitectures by repeatedly establishing the nidus morphology 10,000 times, then randomly sampling a distinct angioarchitecture from the SBM and separately performing hemodynamic simulations on each angioarchitecture.

2.3. Hemodynamic simulations

The flow through the AVM network was calculated according to Kirchhoff's circuit laws: (1) the algebraic sum of the currents at any node should be zero, that is, flow into a node must equal flow out of a node; and (2) the algebraic sum of the changes in potential (that is, the pressure gradient) found in a closed traversal should also be zero. Within a current loop, when a resistor was traversed in the direction of the current, the change in pressure was considered $-QR_v$; and in the opposite direction it was considered $+ QR_v$. When a source of pressure was traversed in the direction of the pressure increase, the change in pressure was considered $+\Delta P$; and in the opposite direction it was considered $-\Delta P$. This provided a system of linear equations relating flow, pressure, and resistance. These equations were represented in matrix form,

$$\Delta\Delta P = R_v Q \quad (2)$$

ΔΔP is a column vector of the pressure differences accumulated over each distinct closed traversal over vessels. ΔΔP also included several zero-valued entries corresponding to each node in the fluidic network. Q is a column vector of all of the vessel flow rates. R_v is a matrix with elements that are either linear combinations of various vessel resistances or the values $\pm$ 1. R_v is constructed so that each line of matrix equation (2) describes the sum of current entering a particular node as zero (Kirchhoff's 1st Law) or is the Hagen–Poiseuille equation for a particular closed traversal over vessels (Kirchhoff's 2nd Law). The flow rates through each vessel were then solved by calculating

$$Q = R_v^{-1} \Delta\Delta P, \quad (3)$$

where R_v^{-1} is the left inverse of R_v. Calculating Q subsequently allowed us to calculate ΔP for each vessel by solving the Hagen–Poiseuille equation. We performed all calculations and simulation steps using Python™ version 2.7 (Delaware, USA).

We assigned appropriate biophysical values to all model vessels (Table 1), and known values of mean intravascular pressure (P_{mean}) to extranidal vessels as described by Hademenos et al. [6], as follows: mean systemic pressure, 74 mm Hg; mean AF1 and AF2 pressures, 47 mm Hg; mean AF3 and AF4 pressures, 50 mm Hg; mean DV1 and DV2 pressures, 17 mm Hg; and mean central venous pressure, 5 mm Hg. The mean pressure at AF3 and AF4 was defined to be slightly higher than that at AF1 and AF2 because of their much smaller size. We used a system of linear equations in matrix form to calculate P_{mean} and flow at each vessel node in the vascular network, including the nidus. More specifically, we used the matrix methods as the first step to solve for Q (as described above). Next, the values of flow in each vessel given by Q were used to solve for the pressure differences in each vessel by using the Hagen-Poiseuille equation. In this sense, the simulations had two steps, solving for the flows in the form of Q using matrix methods, then solving for the pressures using the Hagen-Poiseuille equation. A pseudocode of the simulation algorithm can be found in the Supplementary Data.

We leveraged recent advances in GPU computing to efficiently parallelize our matrix calculations and operations, enabling us to perform the AVM model simulations at unprecedented complexity and speed. This made it possible to simulate 10,000 distinct nidus

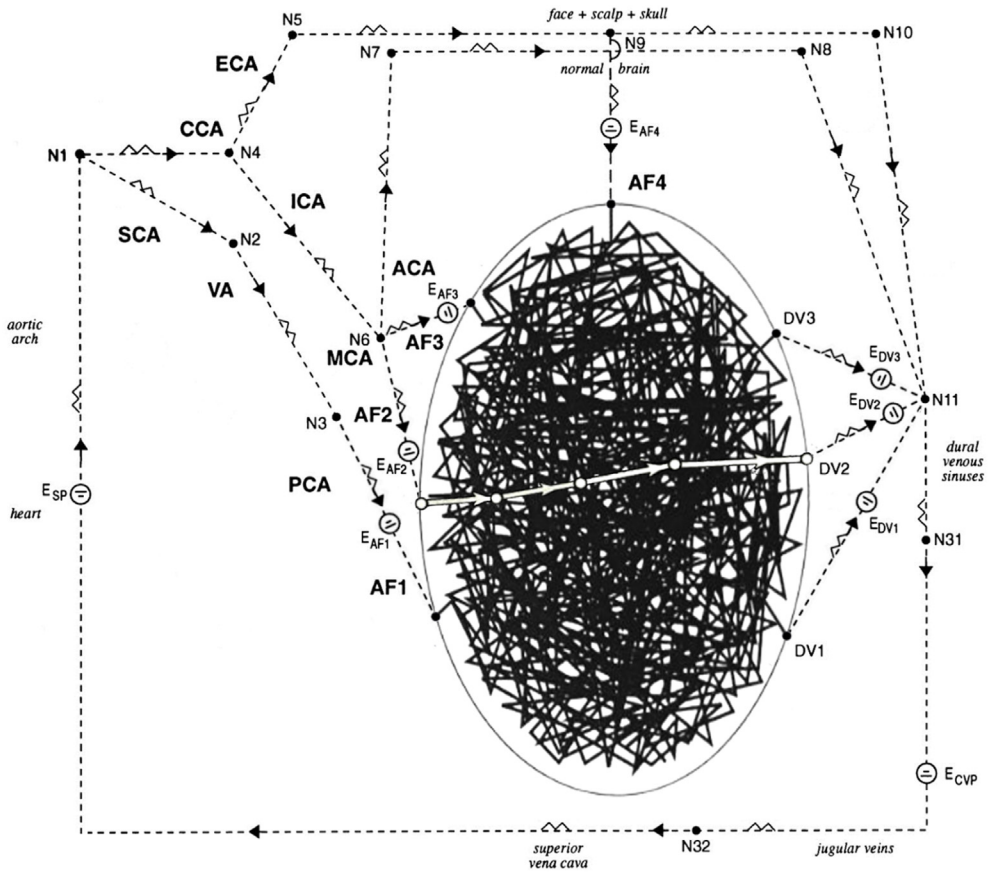

Fig. 1. Schematic of the AVM model, and details of the AVM nidus network. The dense cluster of vessels within the oval is the stochastic angioarchitecture of the nidus, randomly sampled from a stochastic block model at simulation, and consisting of an average of 1000 vessels spanning 57 nodes. AF, arterial feeder; DV, draining vein; CCA, common carotid artery; ECA, external carotid artery; ICA, internal carotid artery; SCA, subclavian artery; VA, vertebral artery; PCA, posterior cerebral artery; ACA, anterior cerebral artery; MCA, middle cerebral artery; E, electromotive force; N, node; CVP, central venous pressure. The intranidal fistula spans AF2 to DV2. Arrowheads indicate direction of flow in simulation.

morphologies within the course of hours, allowing the study of varying nidus geometries. We then mapped these intranidal hemodynamic values onto a graphic representation of the nidus network using graded color scales to indicate hemodynamic ranges.

2.4. Risk of nidus rupture

We also derived an expression for risk of rupture in each vessel as described by Hademenos and Massoud previously [7]. It is commonly believed that on the basis of biomechanical properties of the intranidal vessels, rupture occurs when the cumulative hemodynamic stresses of the vessel wall exceed its elastic modulus.

Equation 10 in the Supplemental Material describes the critical radius of a blood vessel. Any increase or decrease in the state variables that would upset this equality could possibly induce rupture. Evaluation of the risk of rupture is based on the functional distribution of the critical radius with respect to the theoretical blood pressure extremes encountered by the nidus and is given by

$$\text{Risk} = \int_{P_{min}}^{P_{exp}} [Et/P]dP / \int_{P_{min}}^{P_{max}} [Et/P]dP \quad (4)$$

where P_{min} and P_{max} are the central venous pressure (CVP) and the "maximum intranidal pressure", respectively, and P_{exp} is the pressure of the nidus vessel determined at simulation. In this study, $P_{min} = 6.6 \times 10^3$ dyne/cm^2 (equivalent to a CVP of 5 mm Hg). The upper limit of arterial pressure experienced by the nidus microvessels before rupture is likely to occur during considerable systemic hypertension (i.e., blood pressure that is then transmitted to the AFs and the nidus). It has been observed that systemic hypertension to a mean value of 118 mm Hg does not precipitate AVM hemorrhage [8]. The influence of higher levels of systemic hypertension on the propensity of AVMs to rupture is unknown. Therefore, in our calculations it is assumed that the normally low-pressure AFs may reach a maximum value of 74 mm Hg during mean systemic hypertensive levels of 118 mm Hg (derived by assuming a linear relationship between these two parameters) [9]. Therefore, 74 mm Hg (equivalent to 9.8×10^4 dyne/cm^2) was chosen as the upper limit of blood pressure (P_{max}) possibly encountered by nidus vessels before rupture. This value of pressure is acknowledged as a conservative estimate, since it has not been observed clinically or determined experimentally. In reality, selection of this pressure value is of secondary importance for the risk calculations because this does not affect the principles conveyed by our theoretical study. We consider the value of 74 mm Hg to be an adequate approximation for the purpose of our calculations. It is noted that maximal AF pressures obtained by Young et al. on systemic hypertensive challenges reached values close to 74 mm Hg [9].

Because the variables E and t cannot be determined quantitatively from in vivo imaging techniques, they are assumed constant and factored from the equation for risk of rupture. Evaluation of Equation (4) yields the following expression for risk of AVM nidus rupture:

$$\text{Risk} = \ln[P_{exp}/P_{min}]/\ln[P_{max}/P_{min}] \quad (5)$$

The expression given in Equation (5) represents the normalized probability or risk of rupture and is multiplied by 100% to present the results as a percentage of risk of rupture. The denominator or normalization constant is the integrated distribution of critical radii for the maximum possible transnidal pressure gradient. It can be seen that, on a qualitative basis, as the intravascular pressure of the nidus vessels reaches that of the "maximum intranidal pressure," the risk of rupture approaches 100%, implying certain rupture. Conversely, for intravascular pressures closer to that of CVP, the risk of rupture decreases accordingly.

Table 1
Anatomic and biophysical parameters for the blood vessels represented in the biomathematical AVM model, as per Hademenos et al. [6].

Vessel	R (cm)	L (cm)	R_v (dyne s/cm^5)
Cardiovasculature			
N32 – E_{SP} (superior vena cava)	0.750	10.0	3.2
E_{SP} – N1 (aortic arch)	1.000	10.0	1.0
N1 – N2 (subclavian artery)	0.350	10.0	67.9
Head and neck vasculature			
Neck and extracranial circulation	0.350	10.0	67.9
N1 – N4 (common carotid artery)	0.200	10.0	637.5
N4 – N5 (external carotid artery)	CP bed	CP bed	1000000.0
N5 – N9	CP bed	CP bed	1000000.0
N9 – N10	0.125	10.0	4177.9
N31 – N32 (jugular veins)	0.400	20.0	79.7
Intracranial circulation			
N4 – N6 (internal carotid artery)	0.250	20.0	522.0
N2 – N3 (vertebral artery)	0.150	25.0	5037.0
N6 – N7	0.100	10.0	10200.0
N7 – N8	CP bed	CP bed	1000000.0
N8 – N11	0.125	10.0	4177.9
N11 – N31 (dural venous sinuses)	0.250	10.0	261.0
AVM vasculature			
Major arterial feeders			
AF1 (posterior cerebral artery)	0.125	5.2	2210.0
AF2 (middle cerebral artery)	0.150	3.7	745.5
Minor arterial feeders			
AF3 (anterior cerebral artery)	0.025	3.7	15725000.0
AF4 (transdural feeding artery)	0.0125	3.0	12750000.0
Nidus vessels			
Plexiform	0.050	5.0	81600.0
Fistulous	0.100	4.0	4080.0
Draining veins			
DV1	0.250	5.0	130.5
DV2	0.250	5.0	130.5
DV3	0.250	5.0	130.5

*R, vessel radius; L, vessel length; R_v, vascular resistance; N, node; E_{SP}, systemic arterial blood pressure; AF, arterial feeder; DV, draining vein; CP capillary.

2.5. Model parameter sensitivity analysis

We conducted a limited sensitivity analysis of the model by systematically altering two biophysical parameters (vessel length and radius) to study the effects of a possible range of normal variations in AVM biophysical parameters on the behavior of this model and its fidelity to physiological reality. We randomly varied vessel length and radius 1000 times throughout the entire network, sampling from a uniform distribution of values centered on the 'typical' values listed in Table 1, and within a 10% range of these values.

3. Results

Hemodynamic simulations on the model were performed in its baseline state, using 1000 sampled nidus angioarchitectures. Three color-mapped examples of these are presented in Fig. 2. We observed a total intranidal volumetric blood flow ranging from 268 mL/min to 535 mL/min, with a mean 463 mL/min (akin to values obtained in large cerebral AVMs [11]), with markedly increased flow through the intranidal fistula. P_{mean} in the plexiform vessels ranged from 50 to 70 mm Hg with a mean of 57 mm Hg, while P_{mean} in the fistulous vessels ranged from 10 to 40 mm Hg with a mean of 21 mm Hg. The maximum percentage rupture risk among all vessels in the nidus ranged from 0% to 60%, with an average of 29%. The full distributions of these values for the 1000 distinct nidus angioarchitectures are shown in Fig. 3.

The limited sensitivity analysis for 1000 random nidus morphologies sampled from the stochastic block model showed the volumetric blood flow through the AVM nidus ranged from 241 to 682 mL/min. P_{mean} in the plexiform vessels of the nidus ranged from 40 to 70 mm Hg, while P_{mean} ranged from 10 to 50 mm Hg through the fistulous vessels. All these observed ranges were realistic and acceptable, indicating the robustness of the model to small variations in the vessel length and radius parameters used in constructing the model.

4. Discussion

Computational models offer theoretical approaches to analyzing AVM hemodynamics that are otherwise difficult to quantify within or in close proximity to a nidus. The many advantages and limitations of theoretical AVM modeling have been discussed in detail previously (see Supplemental Discussion) [6].

Many biomathematical and computational models have been used previously to study the hemodynamics of AVMs [2–4]. These older models offered a theoretical means of investigating AVM hemodynamics but provided limited information owing to the simplicity of simulated anatomical and physiological AVM characteristics. The models typically involved multicompartmental analysis of nidus vessels arranged independently and in parallel, with invariably one AF and one DV to simplify the modeling process. However, brain AVMs with one AF and one DV are somewhat uncommon [12]. Instead, clinical angiographic examination of AVMs has shown that they are much more often fed and drained by multiple AFs and DVs [12]. Further, the tightly interwoven microvessels contained within the nidus are typically interconnected with many branches, at least bifurcations and trifurcations, making them very dependent on each other and on the hemodynamics at feeding and draining pedicles.

The AVM model developed by Lo [2,13,14] consisted of three linked compartments representing AFs, shunting arterioles, and the core vessels of the AVM draining into the central venous drainage. They simulated hemodynamics within small and large AVMs with results comparable to those observed clinically but neglected the appearance of the DVs. Subsequently, Hecht, Horton, and Kerber extended this concept to simulations of an AVM nidus composed of 1000 nidus vessels [15]. Ornstein et al. introduced a more complex AVM model by considering the influence of inductance, conductance, and autoregulation [16]. They employed an electrical circuit analog to develop a simulated model of an AVM consisting of an AF, DV, and a capillary bed with an encased fistula. Their study modeled the hemodynamic effects of AVM occlusion, thus simulating neurosurgical resection and embolotherapy. In general, these and other ([3,4,17–20]) past models presented with common underlying limitations: 1. the presence of a single AF and either a single DV or neglect of venous drainage; 2. compartmentalized nidus vessels; and 3. representation of the nidus as a single resistance or series of resistances.

Since the concept of electrical networks can serve a unique purpose in hemodynamic modeling of AVMs, this approach was uniquely extended by Hademenos et al. [6] to the characterization of nidus vessels, which are otherwise difficult to study, since they cannot be visualized adequately by current imaging technology (insufficient spatial resolution) and are understood primarily from postmortem and histopathological analysis [21]. Their biomathematical AVM model was constructed to simulate more closely the clinical features and anatomic landmarks typically seen in brain AVMs. The AVM network contained a rudimentary nidal angioarchitecture with a randomly distributed array of 28 interconnected plexiform and fistulous components fed and drained by multiple AFs and DVs. Their computational model was used previously as a theoretical simulator for investigating AVM venous drainage impairment [7], AVM radiosurgery [22], and in simulating a newly proposed embolization technique for brain AVMs [12].

Our more realistic AVM model incorporates new features, including higher intranidal vessel counts and representations of innumerable potential nidus morphologies, the analysis of which is made possible by large-scale, massively parallel data processing using advanced GPU computing. A GPU is used to accelerate applications running on a computer central processing unit by parallelizing of computation and matrix operations. This model is one of a single complex configuration (an advance on prior modeling), and is constructed by incorporating

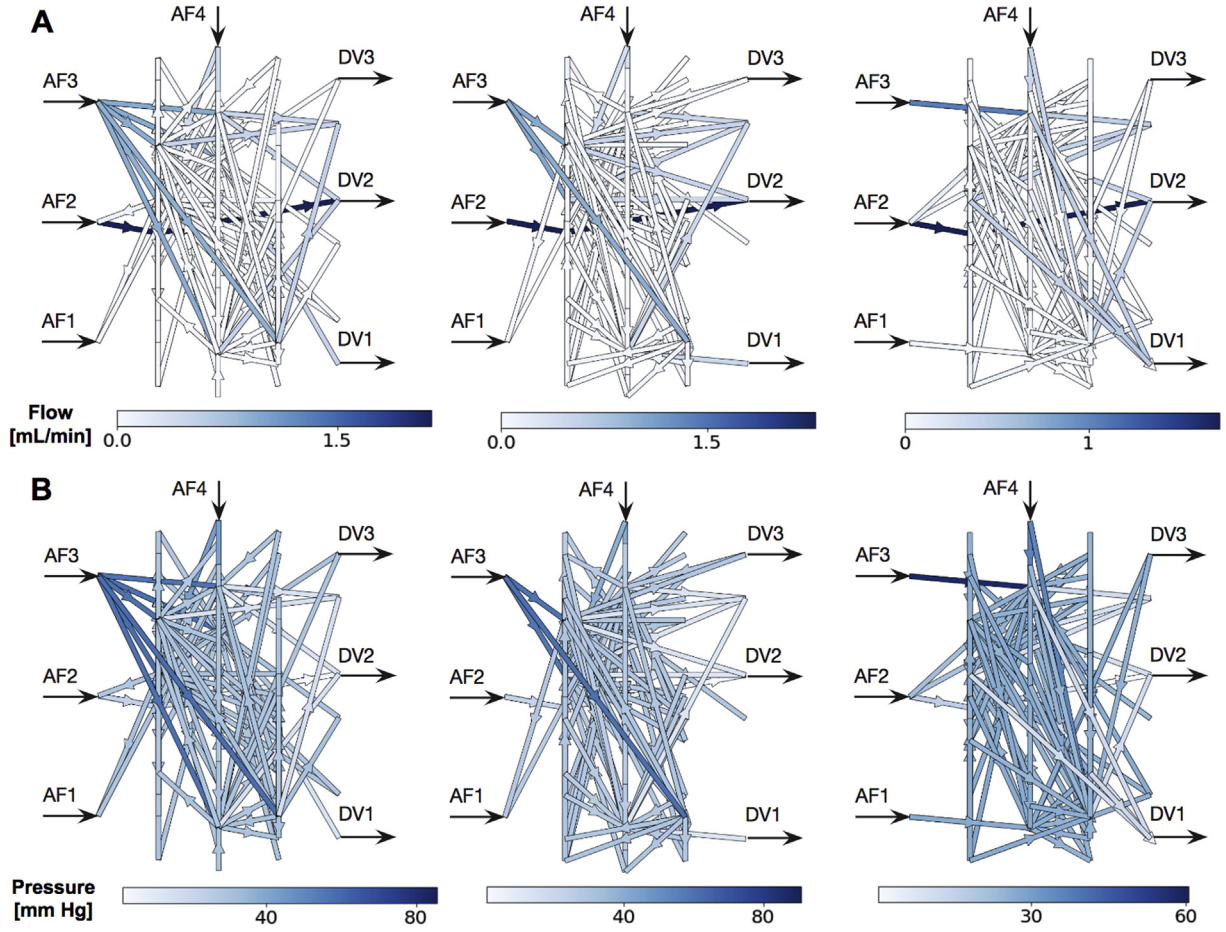

Fig. 2. Hemodynamic simulations of the AVM model. **A.** Simulated intranidal volumetric flow rate through the nidus (color scale in mL/min) of three randomly sampled nidus angioarchitectures. **B.** Simulated intranidal P_{mean} in the same three nidi (color scale in mm Hg). AF, arterial feeder; DV, draining vein.

average published biophysical and hemodynamic parameters. A comprehensive sensitivity analysis of all AVM parameters [10] was beyond the scope of this initial presentation. Importantly, however, we found that the model predicted realistic nidus flow rates, P_{mean} values, and rupture risks when this single network configuration was widely varied, showing that the results observed were not strongly network-dependent or owing to a particular choice of network geometry. Even though we were not able to test more datasets/architectures on our model, the significance of our results indicates generalizability to other datasets/architectures.

This model is attractive in terms of its simplicity, intuitive familiarity (with some resemblance to clinically encountered AVMs), its implemented anatomic features, and ease of its computer simulations. The visual display of results in color-coded graphics superimposed on a theoretical representation of an AVM nidus without a full need for mathematical comprehension of the underlying computer simulations is an additional appeal. There are however several limitations to this modeling process. Firstly, it is entirely theoretical and based on construction and simulation of a theoretical rather than a real human AVM—the data used are not directly obtained from a patient harboring an AVM. Secondly, the precise reasons for why we observed the nidus rupture risk in such discrete distributions, as shown in Fig. 3, is uncertain. To decipher this may require future more detailed multivariate analysis of biophysical and hemodynamic characteristics of this AVM that are beyond the scope of this initial presentation. Additionally, the absence of some concrete data for simulating the nidus portion of the

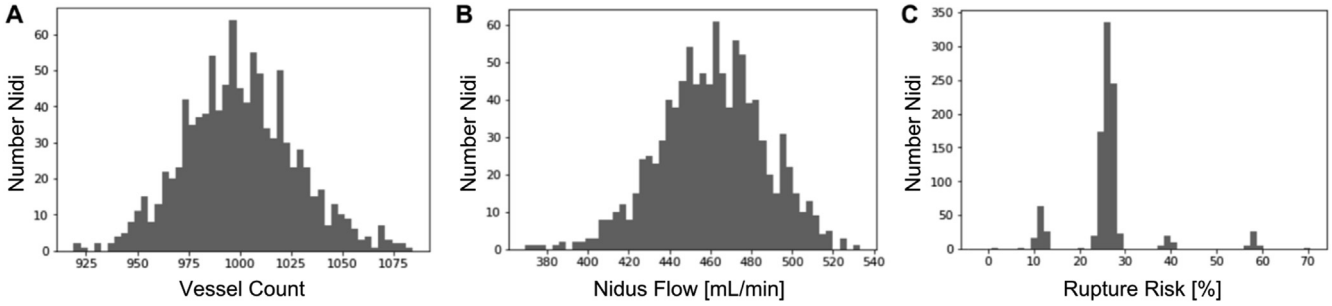

Fig. 3. Characterization of the theoretical AVM model in its baseline state. **A.** Range of number of nidus vessels (1000 on average). **B.** Total intranidal flow (mean of 463 mL/min) **C.** Maximum percentage rupture risk among all vessels of a particular nidus (mean of 29%). Distributions drawn from 1000 distinct nidus angioarchitectures.

model (e.g. nidus vessel length) is an important drawback, which plays precisely into the 'black box' concept that an AVM nidus represents. Therefore, we believe that our modeling should act as a stimulus for further study of human AVM nidus biophysical and morphometric characteristics that could then feedback into, and be implemented in future AVM models that guide clinical decision making. The current work will serve as a useful blueprint for future more ambitious and clinically relevant AVM simulation projects. More specifically, this model should act as a useful template in our future efforts to create a patient-specific AVM simulator and a clinical tool for planning multi-modal AVM therapies and their hemodynamic sequelae.

5. Conclusion

We developed a theoretical AVM model incorporating complex and more realistic morphological and hemodynamic features than in prior models, allowed by parallel data processing using advanced GPU computing. This easy to implement model will be of benefit to clinical and research neuroscientists engaged in study and management of AVM patients.

Declarations of interest

None.

Author contributions

T.F.M. conceived this study. All authors designed the experiments. T.F.M. and H.M.D. supervised the experiments. M.S.J. and T.F.M. performed the experiments. All authors interpreted the results. M.S.J. and T.F.M. wrote the manuscript. All authors reviewed and approved the manuscript, and discussed the results and commented on the manuscript.

Disclosure of funding

This research did not receive any specific grant from funding agencies in the public, commercial, or not-for-profit sectors.

Conflicts of interest

None declared.

Acknowledgements

We are grateful to George Hademenos, PhD, formerly at the Department of Radiological Sciences, UCLA, for initial discussions and help with this AVM model.

Appendix A. Supplementary data

Supplementary data to this article can be found online at https://doi.org/10.1016/j.compbiomed.2019.103416.

References

[1] K. Fukuda, M. Majumdar, H. Masoud, T. Nguyen, A. Honarmand, A. Shaibani, S. Ansari, L.A. Tan, M. Chen, Multicenter assessment of morbidity associated with cerebral arteriovenous malformation hemorrhages, J. Neurointerventional Surg. 9 (2017) 664–668.
[2] E.H. Lo, A hemodynamic analysis of intracranial arteriovenous malformations, Neurol. Res. 15 (1993) 51–55.
[3] E. Gao, W.L. Young, G.J. Hademenos, T.F. Massoud, R.R. Sciacca, Q. Ma, S. Joshi, H. Mast, J.P. Mohr, S. Vulliemoz, J. Pile-Spellman, Theoretical modelling of arteriovenous malformation rupture risk: a feasibility and validation study, Med. Eng. Phys. 20 (1998) 489–501.
[4] Y. Kiran Kumar, S.B. Mehta, M. Ramachandra, Simulation study of hemodynamic in bifurcations for cerebral arteriovenous malformation using electrical analogy, J. Biomed. Phys. Eng. 7 (2017) 143–154.
[5] W.B. Hamby, The pathology of supratentorial angiomas, J. Neurosurg. 15 (1958) 65–75.
[6] G.J. Hademenos, T.F. Massoud, F. Viñuela, A biomathematical model of intracranial arteriovenous malformations based on electrical network analysis: theory and hemodynamics, Neurosurgery 38 (1996) 1005–1014 discussion 1014-1015.
[7] G.J. Hademenos, T.F. Massoud, Risk of intracranial arteriovenous malformation rupture due to venous drainage impairment: a theoretical analysis, Stroke 27 (1996) 1072–1083.
[8] M.D. Szabo, G. Crosby, P. Sundaram, B.A. Dodson, R.N. Kjellberg, Hypertension does not cause spontaneous hemorrhage of intracranial arteriovenous malformations, Anesthesiology 70 (1989) 761–763.
[9] W.L. Young, A. Kader, J. Pile-Spellman, E. Ornstein, B.M. Stein, For the Columbia University AVM Study Project, Arteriovenous malformation draining vein physiology and determinants of transnidal pressure gradients, Neurosurgery 35 (1994) 389–395 discussion 395-6.
[10] G.J. Hademenos, T.F. Massoud, An electrical network model of intracranial arteriovenous malformations: analysis of variations in hemodynamic and biophysical parameters, Neurol. Res. 18 (1996) 575–589.
[11] S. Yamada, S. Thio, R.P. Iacono, B.S. Yamada, F.S. Brauer, W. Hayward, V.J. Morgese, M. Moghtader, Total blood flow to arteriovenous malformations, Neurol. Res. 15 (1993) 379–383.
[12] T.F. Massoud, G.J. Hademenos, Transvenous retrograde nidus sclerotherapy under controlled hypotension (TRENSH): a newly proposed treatment for brain arteriovenous malformations—concepts and rationale, Neurosurgery 45 (1999) 351–363 discussion 363-5.
[13] E.H. Lo, J.I. Fabrikant, R.P. Levy, M.H. Phillips, K.A. Frankel, E.L. Alpen, An experimental compartmental flow model for assessing the hemodynamic response of intracranial arteriovenous malformations to stereotactic radiosurgery, Neurosurgery 28 (1991) 251–259.
[14] E.H. Lo, A theoretical analysis of hemodynamics and biomechanical alterations in intracranial AVMs after radiosurgery, Int. J. Radiat. Oncol. Biol. Phys. 27 (1993) 353–361.
[15] S.T. Hecht, J.A. Horton, C.W. Kerber, Hemodynamics of the central nervous system arteriovenous malformation nidus during particulate embolization: a computer model, Neuroradiology 33 (1991) 62–64.
[16] E. Ornstein, W.B. Blesser, W.L. Young, J. Pile-Spellman, A computer simulation of the hemodynamic effects of intracranial arteriovenous malformation occlusion, Neurol. Res. 16 (1994) 345–352.
[17] S. Nagasawa, M. Kawanishi, S. Kondoh, S. Kajimoto, K. Yamaguchi, T. Ohta, Hemodynamic simulation study of cerebral arteriovenous malformations. Part 2. Effects of impaired autoregulation and induced hypotension, J. Cereb. Blood Flow Metab. 16 (1996) 162–169.
[18] P. Orlowski, F. Al-Senani, P. Summers, J. Byrne, J.A. Noble, Y. Ventikos, Towards treatment planning for the embolization of arteriovenous malformations of the brain: intranidal hemodynamics modeling, IEEE Trans. Biomed. Eng. 58 (2011) 1994–2001.
[19] M.L. Litao, C.P. Pilar-Arceo, G.D. Legaspi, AVM Compartments: do they modulate trasnidal pressures? An electrical network analysis, Asian J. Neurosurg. 7 (2012) 174–180.
[20] X. Lv, Z. Wu, Y. Li, Arteriovenous malformation in the brain: a theoretical study explaining the behavior of liquid embolic agents during endovascular treatment, Neuroradiol. J. 26 (2013) 661–668.
[21] W.B. Hamby, The pathology of supratentorial angiomas, J. Neurosurg. 22 (1957) 65–75.
[22] T.F. Massoud, G.J. Hademenos, A.A. De Salles, T.D. Solberg, Experimental radiosurgery simulations using a theoretical model of cerebral arteriovenous malformations, Stroke 31 (2000) 2466–2477.